CHAPTER NINE

The Hydrogen-Atom Problem and Coulomb Sturmian Functions in Spheroidal Coordinates

Tamaz Kereselidze[1,*], John F. Ogilvie[†,‡]

*Faculty of Exact and Natural Sciences, Tbilisi State University, Tbilisi, Georgia
†Centre for Experimental and Constructive Mathematics, Simon Fraser University, Burnaby, BC, Canada
‡Escuela de Qumica, Universidad de Costa Rica, Ciudad Universitaria Rodrigo Facio, San Jose, Costa Rica
[1]Corresponding author: e-mail address: tamaz.kereselidze@tsu.ge

Contents

Abstract

We survey methods elaborated for the solution of the hydrogen-atom problem in prolate spheroidal coordinates for the discrete spectrum. The expressions of Coulomb spheroidal functions and Coulomb Sturmian functions defined in spheroidal coordinates are collected and presented in a convenient form for their facile application in various calculations. Exploring the properties of spheroidal Sturmians, we show that they are the most appropriate functions for calculations on diatomic molecules.

For the continuous spectrum Coulomb spheroidal functions are obtained through an exact solution of the appropriate one-dimensional equations, which are shown to be Heun's confluent equations. The derived functions are a natural generalization of the well-known Coulomb wave functions of the continuous spectrum obtained in spherical polar coordinates.

Advances in Quantum Chemistry, Volume 77
ISSN 0065-3276
https://doi.org/10.1016/bs.aiq.2018.02.002

© 2018 Elsevier Inc.
All rights reserved.

1. INTRODUCTION

Hydrogen in atomic or plasma form accounts for 9 of 10 atoms in the universe and for about three-quarters of its mass. The solution of the hydrogen-atom problem is hence of such fundamental importance that it warrants solution in all practicable cases. The problem is typically treated in spherical polar and paraboloidal coordinates for both the discrete and continuous spectra.[1] The solution involves separating the spherical or paraboloidal variables so that the amplitude or wave functions are represented as a product of one-dimensional functions.

In addition to spherical polar and paraboloidal coordinates, the Schrödinger equation for a Coulomb field is separable in prolate spheroidal coordinates.[2] A Coulomb center is located at one focus of those spheroidal coordinates; another focus lies at distance R from the Coulomb center and is a dummy center. The separation yields three equations for the three spatial variables, which become the familiar radial and angular equations when R tends to zero, i.e., in spherical polar coordinates. The solutions of the equations with nonzero R might hence be called quasi-radial and quasi-angular functions.

Coulson and Robinson[3,4] made an initial attempt to solve the hydrogen-atom problem in spheroidal coordinates for the discrete spectrum; their important result was a termination of the power series for the one-dimensional functions and a derivation of Coulomb spheroidal functions in a polynomial form. Cook and Fowler[5] applied these techniques to extend the known solutions and to study their application to chemical binding. Using the *hidden symmetry* of the hydrogen atom, Sung and Herschbach[6] derived Coulomb spheroidal functions for eigenstates with $n \leq 4$ and $m \leq 4$, in which n denotes the principal quantum number and m denotes the modulus of the magnetic quantum number. For eigenstates with $m = 0$, Coulomb elliptic functions were obtained and used to study molecular Rydberg states.[7] In Ref. 8 we showed that a simple and straightforward scheme of calculation enables spheroidal functions to be derived in a polynomial form for, in principle, arbitrary eigenstates.

The problem of one Coulomb center in spheroidal coordinates appears not to have been treated for the continuous spectrum; accordingly, Coulomb spheroidal functions corresponding to the continuous spectrum are not yet available in a closed algebraic form. Our purpose is to eliminate this

deficiency in our knowledge. The one-dimensional amplitude functions, we present as a convenient power series, which lead to a pair of three-term recurrence relations for the quasi-angular and quasi-radial functions. The separation parameter is determined from a continued-fraction equation, the roots of which yield these eigenvalues.

The interest in the solution of the hydrogen-atom problem in spheroidal coordinates[9,10] arises because it is closely related to the so-called two-Coulomb-center problem, for which the Schrödinger equation is separable also in spheroidal coordinates.[2] In turn, a knowledge of the wave functions of the discrete and continuous spectrum in algebraic form for an electron moving in the field of two fixed Coulomb centers opens a new possibility to investigate various processes involving ionization and recombination in diatomic systems, occurring in natural and artificial plasmas, the interstellar medium and the terrestrial atmosphere.

Attention to the solution of the hydrogen-atom problem in spheroidal coordinates stimulated interest in Coulomb Sturmian functions derived in prolate spheroidal coordinates. At an early stage of the development of wave mechanics, hydrogen-like amplitude functions were considered to be satisfactory basis functions to build orbitals of many-electron atoms; it was soon revealed, however, that, unless the continuum be included, the hydrogen-like functions form an incomplete set, and thus fail to yield the proper atomic orbitals. To rectify this deficiency, Shull and Löwdin[11] proposed to construct basis functions in such a way as to be complete: i.e., any function obeying the appropriate boundary conditions was expansible in terms of the introduced basis functions. Basis sets of this type have been called a Sturmian basis to emphasize their connection with Sturm–Liouville theory. Coulomb Sturmian functions obtained in spherical polar coordinates have found many applications in atomic physics. The completeness of Coulomb Sturmians combined with their satisfactory properties of convergence makes them suitable to construct amplitude functions of many-electron atoms.[12]

The efficient application of Coulomb Sturmians in atomic physics makes possible the use of this method in molecular calculations. For systems of one electron and many centers, calculations with Coulomb Sturmians are reported in several papers.[13,14] Coulomb Sturmians were used to treat problems involving many centers and many electrons.[15,16] Generalized Sturmian basis functions, their connection to hyperspherical harmonics and their application to solve many-electron problems directly, without the use of the self-consistent-field approximation, are explored elsewhere.[17]

In comparison with numerous applications of Coulomb spherical and paraboloidal Sturmian functions, spheroidal Sturmians have received little attention. In Refs. 18,19, Coulomb spheroidal Sturmians are derived in two limiting cases, at small and large R. The results were obtained on representing the unknown functions in terms of Coulomb spherical (at small R) and Coulomb paraboloidal (at large R) Sturmians. The slight attention to spheroidal Sturmians is attributed to the fact that solutions of the appropriate one-dimensional equations were not recognized to be expressible in terms of known special functions,[3,4] although these equations are now understood to be solvable directly in terms of Heun's confluent functions.[20,21]

The aim of the present work is thus, first, to collect and to present in a convenient form the expressions of Coulomb spheroidal and spheroidal Sturmian functions for their facile application in various calculations and, second, to solve the hydrogen atom problem for the continuous spectrum in spheroidal coordinates and to obtain the spheroidal quasi-radial and quasi-angular functions in an explicit algebraic form. We concentrate on a direct solution of the hydrogen-atom problem, making no use of other and sophisticated methods such as using a hidden symmetry of the hydrogen atom, or a group-theoretical approach. We demonstrate that Coulomb spheroidal functions derived for the discrete spectrum are naturally obtained hybrid functions that reflect the dynamical properties of atomic orbitals, Coulomb spheroidal functions derived for the continuous spectrum are a natural generalization of the well-known Coulomb wave functions of the continuous spectrum obtained in spherical polar coordinates, and Coulomb Sturmian functions defined in spheroidal coordinates are the most appropriate basis functions for calculations on diatomic molecules.

The chapter is organized as follows. After stating our objective, we derive Coulomb spheroidal functions for the discrete and continuous spectrum in Sections 2 and 3, respectively. In Section 4, we present Coulomb Sturmian functions obtained in spheroidal coordinates. In Section 5, an application of the derived function is discussed, before a conclusion in Section 6. Atomic units $(e = m_e = \hbar = 1)$ are used throughout.

2. DISCRETE SPECTRUM

2.1 Basic Equations

We consider a hydrogen-like atom with nuclear charge Z_a. Because the energy spectrum is independent of the system of coordinates in which

electron motion is quantized, the problem is reduced to the derivation of the amplitude functions. In prolate spheroidal coordinates $\xi = (r_a + r_b)/R$, $\eta = (r_a - r_b)/R$, $\varphi = \arctan(y/x)$, the amplitude function is represented as this product of three functions

$$\psi(\xi,\eta,\varphi) = X(\xi)Y(\eta)e^{\pm im\varphi}, \tag{1}$$

in which quasi-radial $X(\xi)$ and quasi-angular $Y(\eta)$ functions depend upon distance R between the centers of spheroidal coordinates; one center, at left, has charge Z_a, and another, a dummy center at right, has $Z_b = 0$. The third function in (1) is $\Phi(\varphi) = e^{\pm im\varphi}/\sqrt{2\pi}$. In the definition of the spheroidal variables, r_a and r_b denote the distances of an electron from those left and right centers of spheroidal coordinates. A surface of constant ξ is an ellipsoid; a surface of constant η is an hyperboloid. These variables ξ and η are thus defined in distinct domains $1 \le \xi < \infty$ and $-1 \le \eta \le 1$ with $0 \le \phi < 2\pi$. In spheroidal functions (1) occur spheroidal quantum numbers n_ξ, n_η, m, of which n_ξ denotes the number of nodes of quasi-radial function $X_{n_\xi m}(\xi)$, and n_η denotes the number of nodes of quasi-angular function $Y_{n_\eta m}(\eta)$.

Substituting (1) into the Schrödinger equation for a hydrogen-like atom, one obtains that $X(\xi)$ and $Y(\eta)$ satisfy these equations

$$\frac{d}{d\xi}\left(\xi^2-1\right)\frac{dX}{d\xi} + \left[\lambda + \frac{ER^2}{2}\left(\xi^2-1\right) + Z_aR\xi - \frac{m^2}{\xi^2-1}\right]X = 0, \tag{2a}$$

$$\frac{d}{d\eta}\left(1-\eta^2\right)\frac{dY}{d\eta} + \left[-\lambda + \frac{ER^2}{2}\left(1-\eta^2\right) - Z_aR\eta - \frac{m^2}{1-\eta^2}\right]Y = 0, \tag{2b}$$

in which appears separation parameter λ, and $E = -Z_a^2/2n^2 \le 0$ is the electron energy.

Representing the quasi-radial and quasi-angular functions as

$$X(\xi) = e^{-\frac{Z_aR}{2n}\xi}\left(\xi^2-1\right)^{\frac{m}{2}}f_1(\xi), \tag{3a}$$

$$Y(\eta) = e^{-\frac{Z_aR}{2n}\eta}(1-\eta^2)^{\frac{m}{2}}f_2(\eta), \tag{3b}$$

and substituting (3a) and (3b) into (2), we obtain equations for unknown functions $f_1(\xi)$ and $f_2(\eta)$,

$$\left(\xi^2-1\right)\frac{d^2f_1}{d\xi^2}+\left[2(m+1)\xi-\frac{Z_aR}{n}(\xi^2-1)\right]\frac{df_1}{d\xi}+\left[\lambda+m^2+m+\frac{Z_aR}{n}(n-m-1)\xi\right]f_1=0, \tag{4a}$$

$$(1-\eta^2)\frac{d^2f_2}{d\eta^2}-\left[2(m+1)\eta+\frac{Z_aR}{n}(1-\eta^2)\right]\frac{df_2}{d\eta}-\left[\lambda+m^2+m+\frac{Z_aR}{n}(n-m-1)\eta\right]f_2=0. \tag{4b}$$

Performing transformations $\xi \to x$ with $x = (1 - \xi)/2$ in (4a) and $\eta \to x$ with $x = (1 + \eta)/2$ in (4b), the above equations become represented in the following form,

$$\left\{x(x-1)\frac{d^2}{dx^2}+[c(x-1)+dx-\mu x(x-1)]\frac{d}{dx}-(a\mu x-\alpha)\right\}f_{1,2}(x)=0, \tag{5}$$

in which

$$\begin{aligned} a&=-n+m+1,\\ c&=d=m+1,\\ \mu&=\mp 2Z_aR/n,\\ \alpha&=\lambda+m^2+m\pm Z_aR(n-m-1)/n. \end{aligned} \tag{6}$$

The upper and lower signs in (6) correspond to the equation for $f_1(x)$ and $f_2(x)$, respectively.

2.2 Coulomb Spheroidal Functions

Eq. (5) is Heun's singly confluent equation.[22,23] As shown in Ref. 3, the solutions of Eqs. (4a) and (4b) are expected to be polynomials; we hence seek the solution of Heun's confluent equation (5) in a polynomial form. Near singular point $x = 0$ ($\xi = 1$ or $\eta = -1$), the regular solutions of Eq. (5) are represented as

$$f_{1,2}(x)=\sum_{i=0}^{\nu} g_i^{(1,2)}x^i,\quad g_0^{(1,2)}=1, \tag{7}$$

in which $g_i^{(1,2)}$ are polynomial coefficients that depend on R; ν defines the degree of the polynomial.

For polynomial (7) to be a solution of Eq. (5), polynomial coefficients $g_i^{(1,2)}$ must satisfy a three-term recurrence relation.[22] When parameters a, c, d, μ and accessory parameter α are defined with (6), this three-term recurrence relation transforms into relation

$$(i+1)(i+m+1)g_{i+1}^{(1,2)} + \left[\nu(2m+\nu+1) \mp \frac{Z_a R}{n}(n-m-1) - h \right.$$
$$\left. -i\left(i+2m+1 \mp \frac{2Z_a R}{n}\right)\right] g_i^{(1,2)} \pm \frac{2Z_a R}{n}(n-m-i)g_{i-1}^{(1,2)} = 0, \tag{8}$$

in which $h = \lambda + (m+\nu)(m+\nu+1)$. Recurrence relation (8) determines the polynomial coefficients in (7) and yields an equation for new separation parameter h. When $R \to 0$, (8) transforms into a two-term recurrence relation that leads to the well-known solutions in spherical polar coordinates.[1]

When $\nu = 0$, $f_{1,2}(x)$ are polynomials of degree zero; recurrence relation (8) converts into equation $\mp (Z_a R/n)(n - m - 1) - h = 0$. To satisfy this equation for arbitrary R, conditions $n = m + 1$ and $h = 0$ must be fulfilled. We thus obtain one spheroidal function $\psi_{n_\xi n_\eta m}$ with quantum numbers $n_\xi = 0$, $n_\eta = 0$, and arbitrary m.

When $\nu = 1$, $f_{1,2}(x)$ are polynomials of first degree; recurrence relation (8) yields two equations for g_1. To satisfy these equations simultaneously h must be the solution of a quadratic equation, which has two real and distinct roots, $h_1 < h_2$. As a result, we obtain two spheroidal functions ψ_{01m} $(h = h_1)$ and ψ_{10m} $(h = h_2)$ with $n = m + 2$.

When $\nu = 2$, $f_{1,2}(x)$ are polynomials of second degree; recurrence relation (8) yields three equations for g_1 and g_2. To satisfy these equations simultaneously h must be the solution of a cubic equation, which has three real and distinct roots, $h_1 < h_2 < h_3$. We obtain three spheroidal functions ψ_{02m} $(h = h_1)$, ψ_{11m} $(h = h_2)$, and ψ_{20m} $(h = h_3)$ with $n = m + 3$. Polynomials of third, fourth, etc. degrees and the equations for appropriate separation parameters are readily evaluated. For given n and m, h is thus a solution of an equation of order $(n - m)$ that has $(n - m)$ real and distinct roots (see Appendix A).

To summarize the above results, we state that, for given m and ν ($\nu = n - m - 1 = 0, 1, 2, \ldots$) Coulomb spheroidal functions are expressible as

$$\psi_{n_\xi n_\eta m} = C_{n_\xi n_\eta m} e^{-\frac{Z_a R(\xi+\eta)}{2n}} \left[(\xi^2-1)(1-\eta^2)\right]^{\frac{m}{2}} \sum_{i=0}^{\nu} g_i^{(1)} \left(\frac{1-\xi}{2}\right)^i \sum_{i=0}^{\nu} g_i^{(2)} \left(\frac{1+\eta}{2}\right)^i e^{\pm im\varphi}, \tag{9}$$

in which $g_0^{(1,2)} = 1$,

$$g_i^{(1,2)} = \frac{1}{i(m+i)}\left\{\left[h-(\nu+1-i)(2m+\nu+i)\pm(\nu+2-2i)\frac{Z_aR}{n}\right]g_{i-1}^{(1,2)} \mp\left[2(\nu+2-i)\frac{Z_aR}{n}\right]g_{i-2}^{(1,2)}\right\}, \quad (i=1,2,\ldots\nu) \tag{10}$$

h is solution of the algebraic equation of order $(n - m)$

$$\left(h\mp\nu\frac{Z_aR}{n}\right)g_\nu^{(1,2)} \mp\frac{2Z_aR}{n}g_{\nu-1}^{(1,2)} = 0, \quad (\nu=0,1,\ldots) \tag{11}$$

and $C_{n_\xi n_\eta m}$ is a normalizing factor. We note that terms with the upper and lower signs vanish in Eq. (11) obtained for h.

We proceed to establish the relation between quantum numbers n_ξ, n_η, m used to specify the electronic states in the general case (with R finite and nonzero) and spherical quantum numbers n, l, m and paraboloidal quantum numbers n_1, n_2, m describing the hydrogen states at $R = 0$ and $R \to \infty$, respectively. Employing that the number of nodal surfaces of $X_{n_\xi m}(\xi)$ and $Y_{n_\eta m}(\eta)$ functions is conserved as R varies,[24] we obtain that $n - l - 1 = n_\xi = n_1$ and $l - m = n_\eta = n_2$. The spheroidal quantum numbers corresponding to degenerate states with given n and m are hence related according to a condition that $n = n_\xi + n_\eta + m + 1$.

Spheroidal functions (9) correspond to a location of a nucleus at the left center of spheroidal coordinates ($\xi = 1, \eta = -1$). For a nucleus located at the right center ($\xi = 1$, $\eta = 1$), quasi-radial function $X_{n_\xi m}(\xi)$ remains unchanged, whereas $\eta \to -\eta$ in quasi-angular function $Y_{n_\eta m}(\eta)$. We thus obtain that Eqs. (9)–(11) define a set of Coulomb spheroidal functions on each center of spheroidal coordinates for the description of localized bonds.

2.3 Properties of Coulomb Spheroidal Functions

Coulomb spheroidal functions (9) with varied m are orthogonal because of factor $\exp(\pm im\varphi)$. The quasi-radial and quasi-angular functions in (9) are defined with Eqs. (2a) and (2b), in which separation parameter λ plays the role of an eigenvalue. The solutions of these equations corresponding to a degenerate level with given n and m are hence mutually orthogonal, provided only that λ are distinct. We recall from Section 2.2 that λ are all real and distinct. Hence $\langle X_{n'_\xi m}|X_{n_\xi m}\rangle = 0$ and $\langle Y_{n'_\eta m}|Y_{n_\eta m}\rangle = 0$ if $n_\xi + n_\eta = n'_\xi + n'_\eta$ and $n'_\xi \neq n_\xi$, $n'_\eta \neq n_\eta$.

Spheroidal functions $\psi_{n_\xi n_\eta m}(\xi,\eta,\varphi)$ can be represented as linear combinations of Coulomb spherical functions $\Psi_{nlm}(r_a, \vartheta_a, \varphi)$. This result is achievable on representing r_b as $r_b = (r_a^2 - 2r_a R\cos\vartheta_a + R^2)^{1/2}$, in which ϑ_a denotes the angle between radius vector $\vec{r}_a$ and axis z, and on representing spheroidal coordinates ξ and η through spherical ones r_a, ϑ_a, φ in $\psi_{n_\xi n_\eta m}(\xi,\eta,\varphi)$. Performing the appropriate calculation, we obtain that, at all separations, $\psi_{n_\xi n_\eta m}(\xi,\eta,\varphi)$ is a linear combination of spherical functions $\Psi_{nlm}(r_a, \vartheta_a, \varphi)$ with principal quantum number n and orbital angular-momentum quantum number $l = m, m+1, \ldots, n-1$. The normalized spheroidal functions are thus expressible as

$$\psi_{n_\xi n_\eta m} = \sum_{l=m}^{n-1} A_{nlm}(R)\Psi_{nlm}(r_a,\vartheta_a,\varphi), \tag{12}$$

in which expansion coefficients are related with the condition $\sum_{l=m} A_{nlm}^2 = 1$. When $R \to 0$, one expansion coefficient is equal to one in (12) whereas the others tend to zero. When $R \to \infty$, spheroidal function $\psi_{n_\xi n_\eta m}$ converts into paraboloidal function $\psi_{n_1 n_2 m}$ with $n_1 = n_\xi$ and $n_2 = n_\eta$. Accordingly, Eq. (12) transforms into the relation between the Coulomb paraboloidal and the Coulomb spherical functions.[1,25] In this limit, $A_{nlm}(\infty) = \langle j_1 j_2 \mu_1 \mu_2 | lm\rangle$ in which $j_1 = j_2 = (n-1)/2$, $\mu_1 = (m + n_\xi - n_\eta)/2$, $\mu_2 = (m - n_\xi + n_\eta)/2$, and $\langle j_1 j_2 \mu_1 \mu_2 | lm\rangle$ is a Clebsch–Gordan coefficient. In Appendix B are presented spheroidal functions $\psi_{n_\xi n_\eta m}(\xi,\eta,\varphi)$ *with arbitrary m and* $n_\xi, n_\eta \le 2$ in terms of spherical functions $\Psi_{nlm}(r_a,\vartheta_a,\varphi)$.

We thus obtain that, with the exception of ψ_{00m}, the derived spheroidal functions are hybrid functions of Coulomb spherical functions Ψ_{nlm} corresponding to the degenerate level with $n = n_\xi + n_\eta + m + 1$ and $E = -Z_a^2/2n^2$. The expression for the probability density is obtained from Eq. (12). Taking into account that spherical function Ψ_{nlm} is a product of radial function $R_{nl}(r_a)$ and spherical harmonic $Y_{lm}(\vartheta_a, \varphi)$, we derive

$$\varrho_{n_\xi n_\eta m}(r_a,\vartheta_a) = \sum_{l,l'=m}^{n-1} A_{nlm}A_{nl'm}R_{nl}(r_a)R_{nl'}(r_a)Y_{lm}^*(\vartheta_a,\varphi)Y_{l'm}(\vartheta_a,\varphi). \tag{13}$$

The radial and angular probability densities are obtained on integrating (13) over either spherical angles ϑ_a and φ or radius r_a, which gives

$$\varrho_{n_\xi n_\eta m}(r_a) = \sum_{l=m}^{n-1} A_{nlm}^2 R_{nl}^2(r_a), \tag{14}$$

for radial density and

$$\varrho_{n_\xi n_\eta m}(\vartheta_a) = \sum_{l=m}^{n-1} A_{nlm}^2 |Y_{lm}(\vartheta_a, \varphi)|^2, \tag{15}$$

for angular density, respectively.

Thus a reduction of symmetry from spherical to axial leads to the coupling of spherical polar orbitals and the formation of hybrid orbitals. The contribution of each spherical orbital within a hybrid orbital depends strongly on distance R from a nucleus to the dummy center, and alters substantially as R varies. At two limiting cases $R \to 0$ and $R \to \infty$, spheroidal functions are purely atomic orbitals, whereas at intermediate R they contain many features intrinsic to diatomic-molecular orbitals. As graphic illustrations of the progression of Coulomb spheroidal functions $\psi_{n_\xi n_\eta m}$ as distance R increases along axis z from the spherical polar limit at $R \to 0$ to the paraboloidal limit as $R \to \infty$, we display plots of surfaces of constant $\psi_{n_\xi n_\eta m}$ functions at a magnitude that is 1/100 of the maximum magnitude. Whereas the functions are expressed in terms of spheroidal coordinates, the figures are plotted in the customary Cartesian coordinates. At any value of R, the surface for function ψ_{000} is a sphere (not shown); for ψ_{010}, ψ_{100}, and ψ_{020} the shapes vary with R as shown in Figs. 1–3.

Fig. 1 shows that, at $R = 0$, the shape of spheroidal orbital ψ_{010} coincides with the shape of spherical polar orbital Ψ_{2p0}.When R increases, this shape alters such that the negative lobe contracts monotonically along axis z, whereas the positive lobe expands along axis z; When $R \gg 1$, the negative lobe is much smaller than the positive lobe. When $R \to \infty$, the shape of spheroidal orbital ψ_{010} resembles strongly the shape of paraboloidal orbital with quantum numbers $n_1 = 0$ and $n_2 = 1$.

At $R = 0$, the shape of spheroidal orbital ψ_{100} has central symmetry as shown in Fig. 2, and coincides with the shape of spherical polar orbital Ψ_{2s0}. When R increases, the spheroidal orbital ψ_{100} has its center clearly displaced along negative axis z. When $R \gg 1$, the shape of spheroidal orbital ψ_{100} resembles strongly the shape of paraboloidal orbital with quantum number $n_1 = 1$ and $n_2 = 0$. According to Figs. 1 and 2, at $R \gg 1$ the shape of spheroidal orbitals ψ_{010} and ψ_{100} are practically identical, but oriented oppositely along axis z.

Fig. 3 shows the shape of spheroidal orbital ψ_{020} as distance R increases from $R = 0$ to $R \gg 1$. At $R = 0$, the shape of this spheroidal orbital coincides

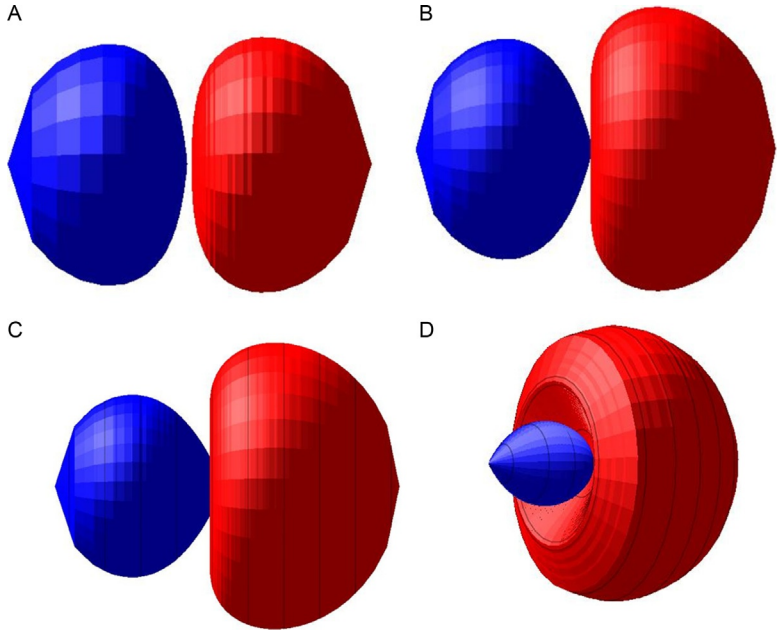

Fig. 1 Coulomb spheroidal function ψ_{010} at distance R from a nucleus to the dummy center: (A) $R = 1/10a_0$, (B) $R = 1a_0$, (C) $R = 2a_0$, and (D) $R = 50a_0(a_0 = \hbar^2/m_e e^2)$.

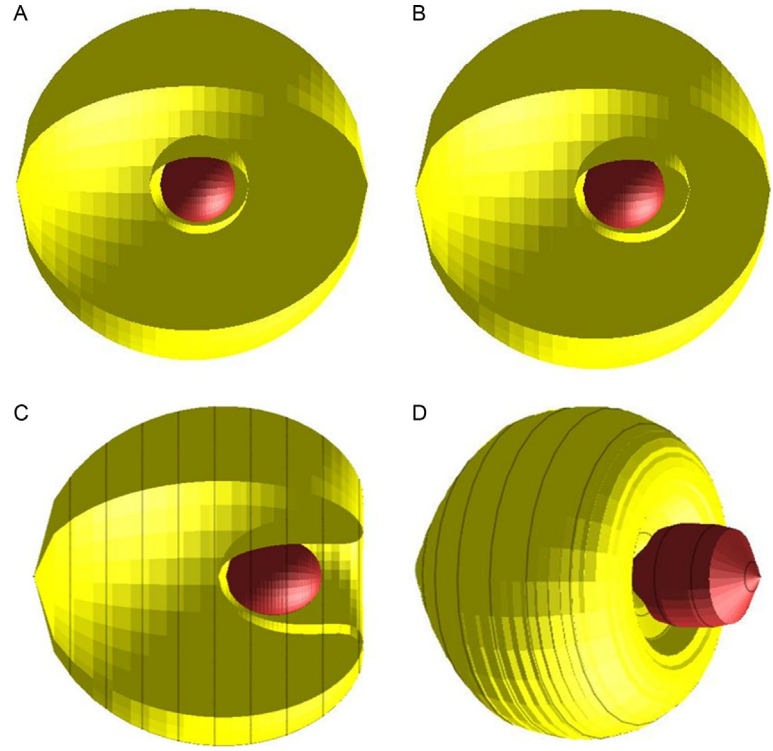

Fig. 2 As in Fig. 1 but for Coulomb spheroidal function ψ_{100}.

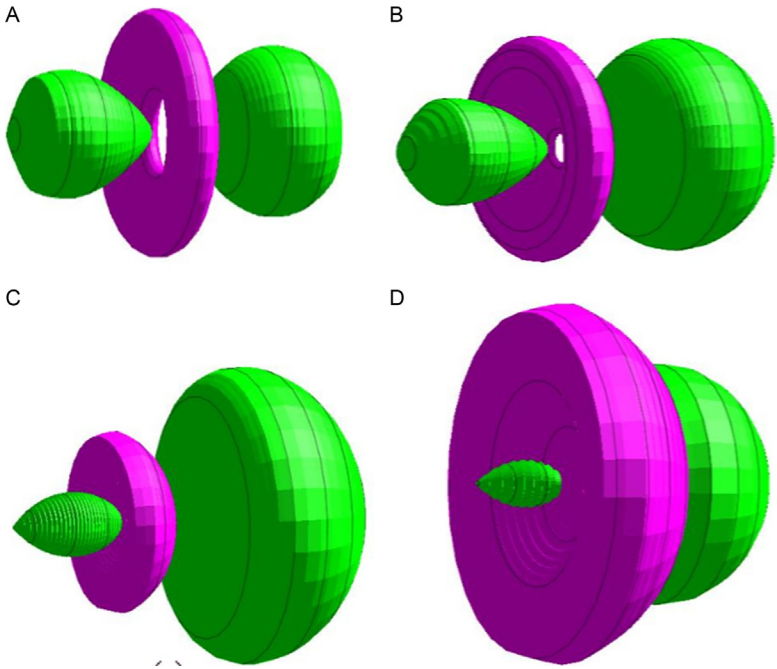

Fig. 3 Coulomb spheroidal function ψ_{020} at distance R from a nucleus to the dummy center: (A) $R = 1/10a_0$, (B) $R = 2a_0$, (C) $R = 5a_0$, and (D) $R = 50a_0$.

with the shape of spherical orbital Ψ_{3d0}. When $R \gg 1$, the shape of spheroidal orbital ψ_{020} resembles strongly the shape of paraboloidal orbital with quantum numbers $n_1 = 0$ and $n_2 = 2$. The tendencies analogous to those shown in Figs. 1–3 are also observable for the other spheroidal orbitals.

Thus for given n and m the most stretched orbital toward the dummy center is an orbital with a maximum number of quasi-angular nodes, whereas the most stretched orbital in the opposite direction is an orbital with a maximum number of quasi-radial nodes. The orbital with $n_\eta = n - m - 1$ is hence a bonding orbital, as distinct from the orbital with $n_\xi = n - m - 1$ that is an antibonding orbital.

3. CONTINUOUS SPECTRUM

For the continuous spectrum the amplitude function is defined by expression (1) in which quasi-radial $X(\xi)$ and quasi-angular $Y(\eta)$ functions are solutions of Eqs. (2a) and (2b) with $E > 0$.

Representing these functions as

$$X(\xi) = e^{i\frac{pR}{2}\xi}\left(\xi^2-1\right)^{\frac{m}{2}} f_1(\xi), \tag{16a}$$

$$Y(\eta) = e^{i\frac{pR}{2}\eta}(1-\eta^2)^{\frac{m}{2}} f_2(\eta), \tag{16b}$$

in which $p = \pm\sqrt{2E}$, and substituting (16a) and (16b) into (2), we obtain equations for unknown functions $f_1(\xi)$ and $f_2(\eta)$.

For $f_1(\xi)$ we obtain

$$\begin{aligned}\left(\xi^2-1\right)\frac{d^2 f_1}{d\xi^2} + \left[2(m+1)\xi + ipR\left(\xi^2-1\right)\right]\frac{df_1}{d\xi} \\ + \left[\lambda + m^2 + m + R(Z_a + ip(m+1))\xi\right] f_1 = 0.\end{aligned} \tag{17}$$

The equation for $f_2(\eta)$ coincides with (17) but with $\xi \to \eta$ and $f_1 \to f_2$. We suppose that functions $f_1(\xi)$ and $f_2(\eta)$ are finite in the entire domain of their definition including the boundaries at $\xi = 1$, $\xi \to \infty$ and $\eta = \pm 1$.

3.1 Quasi-Angular Functions

To begin, we find the eigenvalues and eigenfunctions of quasi-angular equation

$$\begin{aligned}(1-\eta^2)\frac{d^2 f}{d\eta^2} - \left[2(m+1)\eta - ipR(1-\eta^2)\right]\frac{df_2}{d\eta} \\ -\left[\lambda + m^2 + m + R(Z_a + ip(m+1))\eta\right] f_2 = 0.\end{aligned} \tag{18}$$

Using the obtained values for separation parameter λ, we then solve the quasi-radial equation (17).

As for the discrete spectrum, performing transformation $\eta \to x$ with $x = (1 + \eta)/2$, and assuming that

$$\begin{aligned} a &= m + 1 - iZ_a/p, \\ c &= d = m + 1, \\ \mu &= -2ipR, \\ \alpha &= \lambda + m^2 + m - (Z_a + ip(m+1))R, \end{aligned} \tag{19}$$

we obtain Heun's confluent equation (5).

Near singular point $x = 0$ (or $\eta = -1$), the regular solutions of Eq. (5) are represented as a power series,[22]

$$f_2(x) = \sum_{k=0}^{\infty} g_k x^k, \tag{20}$$

in which $g_0 = 1$ and x varies in domain [0, 1].

For expansion (20) to be a solution of Eq. (5), expansion coefficients g_k must satisfy a three-term recurrence relation,

$$A_k g_{k+1} + (B_k - \alpha) g_k + C_k g_{k-1} = 0, \tag{21}$$

with

$$\begin{aligned} A_k &= (k+1)(k+c), \\ B_k &= -k(k+c+d+\mu-1), \\ C_k &= \mu(k+a-1), \end{aligned} \tag{22}$$

and a, c, d, μ, and α defined in (19).

We proceed to calculate separation parameter λ at given p as a function of R. Recurrence relation (21) leads to a continued-fraction equation in α, the roots of which determine these eigenvalues and thereby determine λ. For a practical calculation it is convenient to employ the equation

$$\begin{aligned} \alpha - B_{k_0} - \cfrac{A_{k_0-1} C_{k_0}}{\alpha - B_{k_0-1} - \cfrac{A_{k_0-2} C_{k_0-1}}{\alpha - B_{k_0-2} - \cdots - A_0 C_1/(\alpha - B_0)}} \\ = \cfrac{A_{k_0} C_{k_0+1}}{\alpha - B_{k_0+1} - \cfrac{A_{k_0+1} C_{k_0+2}}{\alpha - B_{k_0+2} - \cdots}}. \end{aligned} \tag{23}$$

This equation is obtained on assuming that $k = k_0$ in (21), determining g_{k_0-1}/g_{k_0} to initiate the calculation, performing transformation $k_0 \to k_0 + 1$ and equating $\left(g_{k_0}/g_{k_0+1}\right)^{-1}$ to g_{k_0+1}/g_{k_0}, which is also determined from (21).

For arbitrary R, the general solution of Eq. (23) can be found only numerically, but in the limiting case, i.e., at $R \ll 1a_0$, (23) can be solved algebraically using an iterative method. A small calculation yields

$$\alpha(R) = -k_0(k_0 + 2m + 1) - [Z_a + ip(m+1)]R + O(R^2). \tag{24}$$

When R tends to zero, the eigenvalues and eigenfunctions of angular equation (18) are well known. In this case $\lambda = -l(l+1)$ in which $l = 0$, 1, 2, … is the quantum number for orbital angular momentum; the eigenfunctions are associated Legendre polynomials $P_l^m(\eta)$. To fulfill this

condition when $R \to 0$, we assume that $k_0 = l - m$ in (24). Thus fixing m and k_0, we define l and thereby determine the associated Legendre polynomial that transforms the solution of quasi-angular equation (18) when $R \to 0$. To specify the states in the general case, i.e., at $R > 0$, it is hence suitable to use quantum numbers k_0 and m. Substituting each root of Eq. (23), $\alpha_{k_0 m}(R)$, into recurrence relation (21) and calculating the expansion coefficients in (20), through Eq. (16b) we determine quasi-angular functions $Y_{k_0 m}(\eta)$ for given R and p.

We have thus two solutions: $Y^{(+)}_{k_0 m}(\eta)$ with $p = \sqrt{2E} > 0$ and $Y^{(-)}_{k_0 m}(\eta)$ with $p = -\sqrt{2E} < 0$. The general solution is a sum of these solutions

$$Y_{k_0 m}(\eta) = \frac{1}{2}\left(Y^{(+)}_{k_0 m}(\eta) + Y^{(-)}_{k_0 m}(\eta)\right). \tag{25}$$

Relation (24) shows that, when $p \to -p$, the real part of $\alpha_{k_0 m}(R)$ does not change, whereas the imaginary part changes sign. The same tendency is observable for the expansion coefficients from recurrence relation (21) when $p \to -p$: $\mathrm{Re} g^{(+)}_k = \mathrm{Re} g^{(-)}_k$ and $\mathrm{Im} g^{(+)}_k = -\mathrm{Im} g^{(-)}_k$. Two terms in (25) hence yield two complex-conjugate functions in $Y_{k_0 m}(\eta)$, which can be represented as

$$Y_{k_0 m}(\eta) = (1-\eta^2)^{m/2} \mathrm{Re}\left\{ e^{i\frac{|p|R}{2}\eta} \sum_{k=0}^{\infty} g^{(+)}_k \left(\frac{1+\eta}{2}\right)^k \right\}. \tag{26}$$

The derived expression shows that the quasi-angular amplitude functions are real functions at all separations R. We thus obtain that $Y_{k_0 m}(\eta)$ with varied k_0 and the same m form a full orthonormal set of amplitude functions that are defined in domain $[-1, 1]$; $\alpha_{k_0 m}(R)$ or $\lambda_{k_0 m}(R)$ form a set of nondegenerate eigenvalues. Quantum number $k_0 = 0, 1, 2, \ldots$ determines the number of nodes of the quasi-angular functions defined in (26).

Employing the expressions derived above, we calculated the eigenvalues and eigenfunctions of the quasi-angular equation for selected states and electron energy $E = \varepsilon_0 = 27.21$ eV. In all calculations Z_a is taken to be unity. Fig. 4 shows $\alpha_{k_0 m}$ as a function of R obtained for $k_0 = 0, 1, 2$ and $m = 0, 1$ through the numerical solution of Eq. (23). We refrain from presenting $\alpha_{k_0 m}(R)$ with $k_0 > 2$ and $m > 1$ because that behavior is analogous to the previous ones.

Concerning the results presented in Fig. 4, we note that, for given quantum numbers k_0, m and parameters p and R, Eq. (23) has multiple roots,

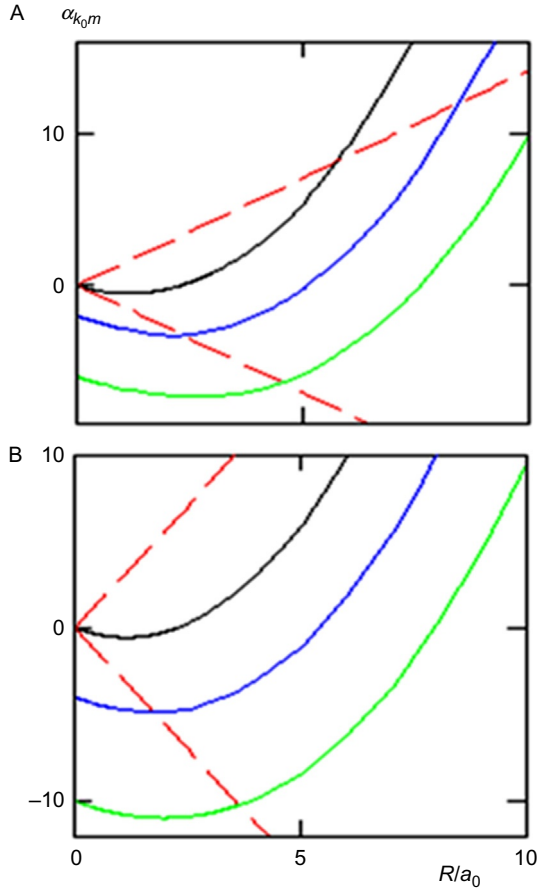

Fig. 4 Parameter $\alpha_{k_0 m}$ as a function of R obtained for $k_0 = 0$, 1, 2 and (A) $m = 0$, (B) $m = 1$ by numerical solution of Eq. (23). *Black curves*—Reα_{0m}, *blue curves*—Reα_{1m}, *green curves*—Reα_{2m}. *Upper red curves*—Im$\alpha_{k_0 m}$ with $p < 0$, *lower red curves*—Im$\alpha_{k_0 m}$ with $p > 0$.

which have complex values. We chose those roots that led to a continuous change of $\alpha_{k_0 m}(R)$ when R varied. Another criterion is a limiting value at $R = 0$, for given k_0 and m, that must be $\alpha_{k_0 m}(0) = -k_0(k_0 + 2m + 1)$ according to Eq. (24). Numerical calculations confirm that the real part of $\alpha_{k_0 m}(R)$ does not change, whereas the imaginary part changes sign when $p \to -p$. An examination of Fig. 4 clearly displays that Im$\alpha_{k_0 m}$ depends linearly on R, which can be interpolated with function

$$\mathrm{Im}\alpha_{k_0 m} = -p(m+1)R \tag{27}$$

at all separations R. Eqs. (19) and (27) show that separation parameter $\lambda_{k_0 m}$ is, correctly, a real function of R. Expression (27) simplifies considerably the finding of the roots of Eq. (23).

Using expression (26), we calculated quasi-angular functions $Y_{k_0 m}(\eta)$ for $k_0 = 0, 1, 2$, $m = 0, 1$ and several R; the results of these calculations are displayed in Fig. 5. Fig. 5A–C shows that $Y_{00}(\eta)$ is a function free of nodes, whereas $Y_{10}(\eta)$ and $Y_{20}(\eta)$ have one and two nodes, respectively, at all separations R. As expected $Y_{00}(\eta)$, $Y_{10}(\eta)$, and $Y_{20}(\eta)$ strongly resemble Legendre polynomials $P_0(\eta) = 1$, $P_1(\eta) = \eta$, and $P_2(\eta) = (3\eta^2 - 1)/2$ at small R. When R increases, the deviation from the Legendre polynomials increases substantially. Quasi-angular function $Y_{01}(\eta)$, which has no node

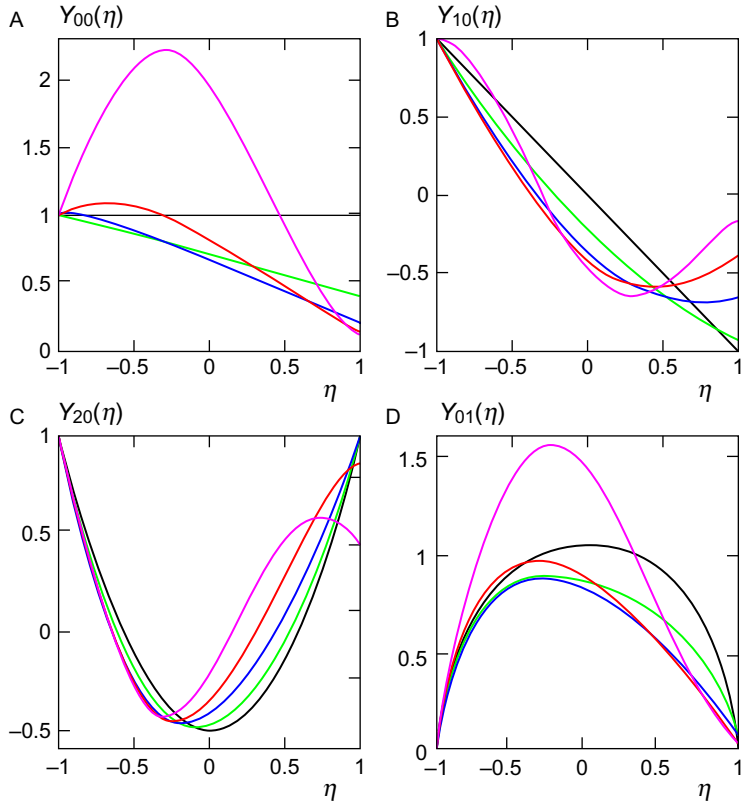

Fig. 5 Quasi-angular functions $Y_{00}(\eta)$, $Y_{10}(\eta)$, $Y_{20}(\eta)$, and $Y_{01}(\eta)$ for $R = 0.01a_0$ (*black curves*), $R = 1.0a_0$ (*green curves*), $R = 2.0a_0$ (*blue curves*), $R = 3.0a_0$ (*red curves*), $R = 5.0a_0$ (*magenta curves*). The functions are normalized according to a condition $Y_{k_0 0}(-1) = 1$.

at any separation R, is displayed in Fig. 5D. This figure shows that $Y_{01}(\eta)$ strongly resembles associated Legendre polynomial $P_1^1(\eta) = (1-\eta^2)^{1/2}$ for $R = 0.01\ a_0$. For all calculated R, expression (26) obtained for quasi-angular function $Y_{k_0 m}(\eta)$ converges rapidly.

3.2 Quasi-Radial Functions

We turn to Eq. (17) for $f_1(\xi)$; this equation is obtained from quasi-radial equation (2a), which is Heun's confluent equation. Following Jaffe,[26] we take

$$f_1(\xi) = (\xi+1)^{\sigma}\sum_{s=0}^{\infty} q_s t^s, \tag{28}$$

in which $q_0 = 1$ and $t = (\xi - 1)/(\xi + 1)$ varies in the domain [0, 1]; σ is a constant quantity to be determined.

Substituting (28) into (17) and making the appropriate calculation, we obtain

$$\left\{ t(1-t)^2\frac{d^2}{dt^2} + \left[2(\sigma-1)(1-t)t + (m+1)(1-t^2) + 2ipRt\right]\frac{d}{dt} + \lambda + m^2 + m \right.$$
$$\left. +\sigma((\sigma-1)t + (m+1)(1+t)) + R\frac{(Z_a + ip(m+1))(1+t) + 2i\sigma pt}{1-t}\right\}\sum_{s=0}^{\infty} q_s t^s = 0. \tag{29}$$

The latter term in Eq. (29) has a singularity at $t = 1$; to remove it, we assume that

$$\sigma = -m - 1 + iZ_a/p. \tag{30}$$

With the singularity at $t = 1$ thus removed, we thereby determine σ.

To fulfill Eq. (29) with σ so defined, expansion coefficients q_s must satisfy a three-term recurrence relation

$$A_s q_{s+1} - B_s q_s + C_s q_{s-1} = 0, \tag{31}$$

in which

$$\begin{aligned} A_s &= (s+1)(s+m+1), \\ B_s &= 2s(s-\sigma-ipR) - \sigma(m+1) + 2i\sigma pR - \alpha_{k_0 m}(R), \\ C_s &= (s-1-\sigma)(s-m-1-\sigma); \end{aligned} \tag{32}$$

$\alpha_{k_0 m}(R)$ are the roots of Eq. (23). Derived recurrence relation (31) and Eqs. (28) and (16a) together yield two solutions of quasi-radial equation (2a):

$X^{(+)}_{Ek_0m}(\xi)$ with $p > 0$ and $X^{(-)}_{Ek_0m}(\xi)$ with $p < 0$. These solutions are complex-conjugate functions because $\mathrm{Re}q_s^{(+)} = \mathrm{Re}q_s^{(-)}$ and $\mathrm{Im}q_s^{(+)} = -\mathrm{Im}q_s^{(-)}$; see Eqs. (30)–(32).

The general solution of Eq. (2a) is a sum of the solutions obtained above, which is a real function at all separations R. One hence writes for the quasi-radial functions defined in spheroidal coordinates that

$$X_{Ek_0m}(\xi) = \frac{(\xi^2-1)^{m/2}}{(\xi+1)^{m+1}}\mathrm{Re}\left\{ e^{i\frac{|p|R}{2}\xi}(\xi+1)^{i\frac{Z_a}{|p|}}\sum_{s=0}^{\infty} q_s^{(+)} t^s \right\}. \tag{33}$$

We proceed to calculate quasi-radial functions $X_{Ek_0m}(\xi)$ for $E = 1.0\ \varepsilon_0$ and several R using expression (33). The convergence in (33) is less rapid than for the quasi-angular functions, especially when R increases. For non-zero and finite R, when distance r_a between the electron and the nucleus increases infinitely, spheroidal variable $\xi = 2r_a/R \to \infty$.[2] In this limit Eq. (2a) transforms into the radial equation obtained in spherical polar coordinates. When $\xi \to \infty$, the solution of quasi-radial equation (2a) must hence coincide with the solution of the familiar radial equation. We apply this condition to find the quasi-radial function in the asymptotic region, i.e., in the region in which $\xi \gg 1$. Fig. 6 shows $(\xi + 1)X_{E00}(\xi)$ as a function of ξ; the same figure shows radial function,[1]

$$\begin{aligned} r_a R_{pl}(r_a) &= \sin\left(pr_a + \frac{Z_a}{p}\ln 2pr_a - \frac{\pi}{2}l + \delta_l \right), \\ \delta_l &= \arg\Gamma(l+1-iZ_a/p), \end{aligned} \tag{34}$$

in which r_a is replaced with $R\xi/2$, l is replaced with $k_0 + m$ and $p = \sqrt{2E}$. Fig. 6A displays that in the asymptotic region the depicted functions have the same phases but different amplitudes. Fig. 6B shows functions $(\xi + 1)X_{E00}(\xi)$ and $r_aR_{p0}(r_a)$ but with equalized amplitudes in the far asymptotic region. Fig. 6B clearly displays that $(\xi + 1)X_{E00}(\xi)$ transforms into $r_aR_{p0}(r_a)$ when ξ increases. This tendency is observable for the quasi-radial functions with quantum numbers other than $k_0 = 0$ and $m = 0$.

We thus obtain that, for finite ξ, the quasi-radial functions are defined with expression (33), whereas, when $\xi \to \infty$, $X_{Ek_0m}(\xi)$ become represented in the familiar form

$$X_{Ek_0m}(\xi) \to \frac{C_{k_0m}}{\xi}\sin\left(\frac{pR}{2}\xi + \frac{Z_a}{p}\ln pR\xi - \frac{\pi}{2}(k_0+m) + \delta_{k_0m} \right), \tag{35}$$

in which C_{k_0m} is a normalizing factor, $\delta_{k_0m} = \arg\Gamma(k_0 + m + 1 - iZ_a/p)$ is the Coulomb phase shift and $\Gamma(x)$ is the gamma function.

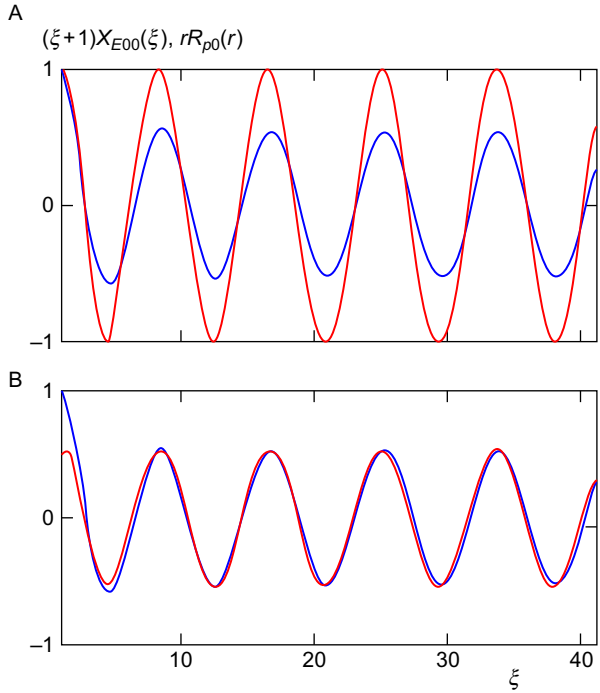

Fig. 6 Functions $(\xi + 1)X_{E00}(\xi)$ (*blue curves*) and $r_aR_{p0}(r_a)$ with $r_a = R\xi/2$ (*red curves*) as a function of ξ. The amplitudes are equalized, (A) at $\xi = 1$ and (B) at $\xi = 38$; $R = a_0$.

In Fig. 7, we demonstrate quasi-radial amplitude functions $X_{E00}(\xi)$ calculated for $R/a_0 = 0.5$ and 1.0. The functions are plotted using expression (33) for $\xi < 38/R$ and expression (35) for $\xi > 38/R$; in (35) the normalizing factor is determined on equating the amplitudes at the boundary of two regions. Fig. 7 shows that the quasi-radial functions are oscillatory at all separations R but with a decreasing amplitude; the frequency of oscillation increases when R increases.

4. COULOMB STURMIAN BASIS IN SPHEROIDAL COORDINATES

The main characteristics of the Coulomb Sturmian basis become evident by reference to the hydrogenic basis. By definition, the Coulomb Sturmian functions ψ satisfy this equation,[15,16]

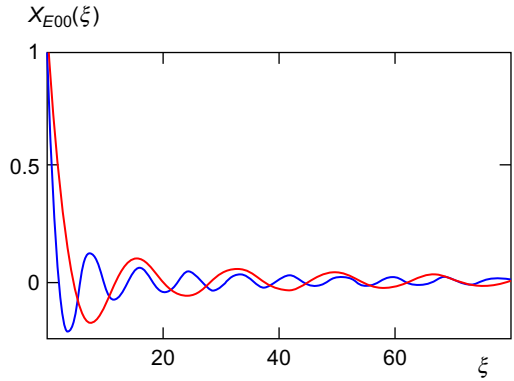

Fig. 7 Quasi-radial functions $X_{E00}(\xi)$ for $R = 0.5a_0$ (*red curve*) and $R = 1.0a_0$ (*blue curve*). The functions are normalized according to condition $X_{E00}(1) = 1$.

$$\left(-\frac{1}{2}\Delta - \frac{Z_a}{r_a} - E\right)\psi = 0, \tag{36}$$

in which $E = -\kappa^2/2 < 0$ is a fixed parameter, $Z_a = n\kappa$ and $n = 1, 2, \ldots$. We seek the solutions of Eq. (36) in prolate spheroidal coordinates ξ, η, φ.

On presenting ψ as a product of three functions $\psi = X(\xi)Y(\eta)e^{\pm im\varphi}$ equation (36) becomes expressed in this form,

$$\frac{d}{d\xi}\left(\xi^2 - 1\right)\frac{dX}{d\xi} + \left[\lambda - \frac{k^2R^2}{4}\left(\xi^2 - 1\right) + nkR\xi - \frac{m^2}{\xi^2 - 1}\right]X = 0, \tag{37a}$$

$$\frac{d}{d\eta}\left(1 - \eta^2\right)\frac{dY}{d\eta} + \left[-\lambda - \frac{k^2R^2}{4}\left(1 - \eta^2\right) - nkR\eta - \frac{m^2}{1 - \eta^2}\right]Y = 0. \tag{37b}$$

Here λ is a separation parameter, energy $E = -Z_a^2/2n^2$ is the same for all solutions and charge Z_a is chosen to make the solutions isoenergetic. Eqs. (37a) and (37b) coincide with Eqs. (2a) and (2b) in which E is replaced with $-\kappa^2/2$ and Z_a with $n\kappa$. The approach elaborated in Section 2.2 for the solution of Eqs. (2a) and (2b) might hence be employed for the solution of Eqs. (37a) and (37b). Representing $X(\xi)$ and $Y(\eta)$ as

$$X(\xi) = e^{-\frac{\kappa R}{2}\xi}\left(\xi^2 - 1\right)^{\frac{m}{2}} f_1(\xi), \tag{38a}$$

$$Y(\eta) = e^{-\frac{\kappa R}{2}\eta}(1 - \eta^2)^{\frac{m}{2}} f_2(\eta), \tag{38b}$$

we obtain for unknown functions $f_1(\xi)$ and $f_2(\eta)$ equations (4a) and (4b) in which Z_a/n is replaced with κ.

Performing transformations $\xi \to x$ with $x = (1 - \xi)/2$ in (4a) and $\eta \to x$ with $x = (1 + \eta)/2$ in (4b), we obtain Heun's confluent equation (5), in which

$$\begin{aligned} &a = m + 1 - n, \\ &c = d = m + 1, \\ &\mu = \mp 2\kappa R, \\ &\alpha = \lambda + m^2 + m \pm \kappa R(n - m - 1). \end{aligned} \tag{39}$$

The upper and lower signs in (39) correspond to the equations for $f_1(\xi)$ and $f_2(\xi)$, respectively.

In accordance with the approach developed in Section 2.2, we represent unknown functions $f_{1,\,2}(x)$ as

$$f_{1,2}(x) = \sum_{i=0}^{\nu} d_i^{(1,2)} x^i, \quad d_0^{(1,2)} = 1. \tag{40}$$

Here $d_i^{(1,2)}$ are polynomial coefficients that must satisfy a three-term recurrence relation (8) in which Z_a/n is replaced with κ. The further derivation is analogous to the derivation of Coulomb spheroidal functions in Section 2.2. As a result, we obtain for Coulomb Sturmian functions defined in prolate spheroidal coordinates that

$$\psi_{n_\xi n_\eta m} = C_{n_\xi n_\eta m} e^{-\frac{\kappa R(\xi+\eta)}{2}} \left[(\xi^2 - 1)(1 - \eta^2)\right]^{\frac{m}{2}} \sum_{i=0}^{\nu} d_i^{(1)} \left(\frac{1-\xi}{2}\right)^i \sum_{i=0}^{\nu} d_i^{(2)} \left(\frac{1+\eta}{2}\right)^i e^{\pm im\varphi}, \tag{41}$$

in which $d_0^{(1,2)} = 1$,

$$\begin{aligned} d_i^{(1,2)} = \frac{1}{i(m+i)} \{ &[h - (\nu + 1 - i)(2m + \nu + i) \pm (\nu + 2 - 2i)\kappa R] d_{i-1}^{(1,2)} \\ &\mp [2(\nu + 2 - i)\kappa R] d_{i-2}^{(1,2)} \Big\}, \qquad (i = 1, 2, \ldots, \nu) \end{aligned} \tag{42}$$

h is solution of the algebraic equation of order $(n - m)$,

$$(h \mp \nu\kappa R) d_\nu^{(1,2)} \mp 2\kappa R d_{\nu-1}^{(1,2)} = 0, \quad (\nu = 0, 1, \ldots) \tag{43}$$

and $C_{n_\xi n_\eta m}$ is a normalizing factor; n_ξ and n_η denote the number of nodes of functions $X_{n_\xi m}(\xi)$ and $Y_{n_\eta m}(\eta)$, respectively; these quantum numbers are related by the condition $n = n_\xi + n_\eta + m + 1$. The terms with the upper

and lower signs vanish in Eq. (43) obtained for h. For the states with arbitrary m and n_ξ, $n_\eta \leq 2$ spheroidal Sturmians are presented in Appendix C.

Spheroidal Sturmian functions (41) with varied m are orthogonal because of factor $\exp(\pm im\varphi)$. Moreover, $\langle X_{n'_\xi m}|X_{n_\xi m}\rangle = 0$ and $\langle Y_{n'_\eta m}|Y_{n_\eta m}\rangle = 0$ if $n_\xi + n_\eta = n'_\xi + n'_\eta$ and $n'_\xi \neq n_\eta$, $n'_\xi \neq n_\eta$ (see the discussion at the beginning of Section 2.3). These properties, characteristic of Coulomb spheroidal functions, are intrinsic also for spheroidal Sturmians.

The above derived spheroidal Sturmian functions $\psi_{n_\xi n_\eta m}$ correspond to the location of a nucleus at the left center of spheroidal coordinates ($\xi = 1$, $\eta = -1$). If a nucleus be located at the right center ($\xi = 1$, $\eta = 1$), $X_{n_\xi m}(\xi)$ remains unchanged, whereas $\eta \to -\eta$ in $Y_{n_\eta m}(\eta)$.

5. APPLICATION

Several algorithms have been elaborated to calculate the energy terms and amplitude functions of the $Z_a e Z_b$ quasi-molecule—the system formed of two nuclei with charges Z_a, Z_b, and an electron, for both the same[27,28] and disparate[29,30] nuclei. These algorithms enable us to calculate numerically the characteristics of a $Z_a e Z_b$ quasi-molecule with a given accuracy. Hence $Z_a e Z_b$ is an ideal system for the estimation of the efficiency of spheroidal Sturmian functions in diatomic-molecular calculations. Despite the elaborated algorithms for the $Z_a e Z_b$ system, attempts to find bases leading to rapid convergence in molecular calculations are continuing (see Refs. 31,32 and references therein).

The amplitude function of an electron moving in the field of two fixed nuclei with charges Z_a and Z_b is represented as follows:

$$\Psi(\xi,\eta,\varphi) = \chi(\xi,\eta)e^{\pm im\varphi}. \tag{44}$$

Substituting (44) into the appropriate Schrödinger equation, one obtains that $\chi(\xi, \eta)$ satisfies the equation

$$\begin{aligned}\Bigg[&\frac{\partial}{\partial\xi}(\xi^2-1)\frac{\partial}{\partial\xi} + \frac{\partial}{\partial\eta}(1-\eta^2)\frac{\partial}{\partial\eta} + \frac{R^2\varepsilon}{2}(\xi^2-\eta^2)\\ &+(Z_a+Z_b)R\xi-(Z_a-Z_b)R\eta-\frac{m^2}{\xi^2-1}-\frac{m^2}{1-\eta^2}\Bigg]\chi(\xi,\eta)=0,\end{aligned} \tag{45}$$

in which $\varepsilon(R)$ is the electron energy.

We introduce the Coulomb Sturmian basis as functions in two sets $\left\{X_{n_\xi m}(\xi)Y^a_{n_\eta m}(\eta)e^{\pm im\varphi}\right\}$ and $\left\{X_{n_\xi m}(\xi)Y^b_{n_\eta m}(\eta)e^{\pm im\varphi}\right\}$, in which the former set corresponds to the location of the nucleus with charge Z_a at the left focus and the latter corresponds to the location of the nucleus with charge Z_b at the right focus of spheroidal coordinates. Our calculating scheme is based on an expansion of function $\chi(\xi, \eta)$ over the basis introduced above. We represent $\chi(\xi, \eta)$ at all separations as

$$\chi = \sum_{n=m+1}^{\infty} \sum_{n_\xi=0}^{n-m-1} \left(C^a_{nn_\xi}(R) X_{n_\xi m}(\xi) Y^a_{n_\eta m}(\eta) + C^b_{nn_\xi}(R) X_{n_\xi m}(\xi) Y^b_{n_\eta m}(\eta) \right), \tag{46}$$

in which $C^{a,b}_{nn_\xi}(R)$ are the expansion coefficients and $n_\eta = n - n_\xi - m - 1$.

We proceed to assume that $\varepsilon = -\kappa^2/2$ in Eq. (45) and that the number of Coulomb Sturmians on each nucleus is restricted. Substituting (46) into (45) and performing the appropriate calculations, we obtain the equations in a finite system for the unknown expansion coefficients. The condition that the determinant of the coefficients of the unknowns vanishes gives the equation for κ and thereby determines the electronic energy. Using the derived equations, we calculated the electronic energies for some low-lying states of the hydrogen molecular ion H_2^+[20] and compared with the analogous ones obtained on employing the Coulomb Sturmian basis set defined in spherical polar coordinates.[15] In our calculations, we restricted a basis size to ten Sturmians because the same number of basis functions on each nucleus has been used in Ref. 15.

Table 1 shows that, at internuclear distances $R > 3a_0$, when the interaction of an electron with its own nucleus is much larger than the interaction with another nucleus, the electronic energies calculated for the ground state in Refs. 15 and 20 coincide. When the interaction of an electron with both nuclei attains the same order of magnitude, i.e., at intermediate and small internuclear distances, $R < 3a_0$, the results obtained in the basis of spheroidal Sturmians are much nearer the exact ones.[27] The difference between the data presented in the third and fourth columns does not exceed $6 \times 10^{-5}\varepsilon_0$ at all separations, whereas for data given in the second column the difference is $\sim 1 \times 10^{-3}\varepsilon_0$. Examenation of Table 2 shows the same tendency: the difference between the exact electronic energies and calculated in Ref. 20 with ten basis functions on each nucleus does not exceed $3 \times 10^{-6}\varepsilon_0$ at all separations, whereas for the electronic energies obtained in Ref. 15 this difference is $5 \times 10^{-3}\varepsilon_0$.

Table 1 Electronic Energy $\varepsilon(R)/\varepsilon_0$ as a Function of Internuclear Distance R for the Ground State $1s\sigma_g$ of H_2^+

R/a_0	Data From Ref. 15	Data From Ref. 20	Exact Data[27]
0.1	−1.97822	−1.978242	−1.978242
0.2	−1.92846	−1.928620	−1.928620
0.4	−1.80006	−1.800753	−1.800754
0.6	−1.67030	−1.671421	−1.671485
0.8	−1.55305	−1.554435	−1.554480
1.0	−1.45032	−1.451755	−1.451786
2.0	−1.10220	−1.102614	−1.102634
3.0	−0.910878	−0.910879	−0.910896
4.0	−0.796074	−0.796074	−0.796085
5.0	−0.724413	−0.724413	−0.724420
6.0	−0.678631	−0.678631	−0.678636
8.0	−0.627569	−0.627569	−0.627570
10.0	−0.600578	−0.600578	−0.600579
15.0		−0.566716	−0.566716

Table 2 Electronic Energy $\varepsilon(R)/\varepsilon_0$ as a Function of Internuclear Distance R for the First Excited State $2p\sigma_u$ of H_2^+

R/a_0	Data From Ref. 15	Data From Ref. 20	Exact Data[27]
0.1	−0.500613	−0.500667	−0.500667
0.2	−0.502489	−0.502677	−0.502677
0.4	−0.509921	−0.510784	−0.510784
0.6	−0.522165	−0.524310	−0.524310
0.8	−0.538910	−0.542746	−0.542746
1.0	−0.559748	−0.564814	−0.564814
2.0	−0.667529	−0.667531	−0.667534
3.0	−0.701418	−0.701417	−0.701418
4.0	−0.695551	−0.695550	−0.695551
5.0	−0.677292	−0.677292	−0.677292
6.0	−0.657311	−0.657311	−0.657311
8.0	−0.623606	−0.623606	−0.623606
10.0	−0.599901	−0.599901	−0.599901

The most striking feature of Rydberg states of long-range diatomic molecules predicted in Ref. 33 is that some molecular Rydberg states possess large electric-dipolar moments, which, in any long-lived molecular state, presents a promising opportunity for manipulation and control through the application of an electric field. A simple model of these molecules has been elaborated: Rydberg states are described with a sum of degenerate Coulomb elliptic wave functions; the attraction between a weakly bound electron and a ground-state atom is described with a short-range potential.[7] In this way, many qualitative features have been understood. The present work shows that to obtain more precise, quantitative results, Rydberg states must be described with Coulomb Sturmian functions defined in spheroidal coordinates; the attraction between a weakly bound electron and two atomic cores should be treated using a realistic potential.

6. CONCLUSION

Our treatment of the hydrogen atom in prolate spheroidal coordinates demonstrates that Coulomb spheroidal functions are related to the solutions of Heun's confluent equation, which enables us to present Coulomb spheroidal functions in a closed algebraic form. Unlike hydrogen molecular ion H_2^+, for which the wave functions are not expressible in a polynomial form, the wave functions for the hydrogen atom in spheroidal coordinates are expressible as the polynomial solutions of Heun's confluent equation. For given principal quantum number n and magnetic quantum number m quasi-radial $X_{n_\xi m}(\xi)$ and quasi-angular $Y_{n_\eta m}(\eta)$ wave functions are polynomials of order $n - m - 1$. Coulomb spheroidal functions with different n and m but the same $n - m$ or $n_\xi + n_\eta$ are thus products of two similar polynomials defined in distinct regions of variables ξ and η, as follows from Eq. (9).

We explore the properties of spheroidal orbitals; for $R > 0$ they are hybrid orbitals composed of spherical wave functions. An important result is that the angular probability density depends on the distance from a nucleus to the dummy center, and varies substantially with R. For given n and m, the orbital most stretched toward the dummy center is an orbital with quasi-angular nodes of maximum number, whereas the orbital most stretched in the opposite direction is an orbital with quasi-radial nodes of maximum number. The characteristic feature of Coulomb spheroidal functions is thus the development of preferred directions around an atom, i.e., the bond directions. These features reveal the great advantage of a Coulomb spheroidal basis over a Coulomb spherical basis in calculations on diatomic molecules.

Coulomb Sturmian functions defined in spherical polar coordinates have long been used for diatomic-molecular calculations. Our work here presents, in a convenient form, Coulomb Sturmians defined in spheroidal coordinates, and demonstrates the possibility of applying these functions for molecular calculations. The obtained results show that, in comparison with Coulomb Sturmians defined in spherical coordinates, the application of Coulomb Sturmian functions derived in spheroidal coordinates substantially speeds convergence and brings the calculated results nearer the exact ones. We attribute this improvement to the fact that spheroidal Sturmians reproduce the behavior of one-electron diatomic-molecular orbitals better than other amplitude functions of exponential type. An important fact is that all relevant integrals are pure functions of parameter kR, in which k is the exponent common to the basis functions and R is internuclear distance. Moreover, the integrals can be calculated analytically once and for all, with kR and nuclear charges Z_a and Z_b as parameters. These advantages enable us to state that Coulomb Sturmian functions defined in spheroidal coordinates are the most appropriate basis functions for diatomic-molecular calculations.

The problem of a hydrogen-like ion is solved in prolate spheroidal coordinates for the continuous spectrum. The one-dimensional equations obtained after separation of the variables in the temporally independent Schrödinger equation are reduced to Heun's confluent equations; the eigenvalues and eigenfunctions of these equations are found in a closed algebraic form. For small distances R between the foci of spheroidal coordinates, the real part of eigenvalues is a linearly decreasing function of R, which then increases rapidly when R increases. The imaginary part of α is a linearly decreasing or increasing function of R at all separations. As shown in Section 3.1, expansion (26) converges rapidly for nonzero and finite R. Expression (26) obtained for quasi-angular function $Y_{k_0 m}(\eta)$ is hence valid for diverse distances R between the foci of spheroidal coordinates. In expansion (33) the convergence is less rapid, especially when R increases; expression (33) derived for quasi-radial function $X_{Ek_0 m}(\xi)$ is consequently valid at small R. When $R > a_0$, the problem of finding spheroidal quasi-radial functions corresponding to the continuous spectrum requires an alternative treatment; work on this problem is in progress.

As mentioned in the introduction, one- and two-Coulomb-center problems in prolate spheroidal coordinates are mathematically similar. This fact enables us to state that the approach elaborated in the present work for the hydrogen-like ion might be efficiently employed for the algebraic solution of the two-Coulomb-center problem for the continuous spectrum.

APPENDIX A

The quadratic equation for $h(R)$ is

$$h^2 - 2(m+1)h - \left(\frac{Z_a R}{n}\right)^2 = 0. \tag{A.1}$$

The cubic equation for $h(R)$ has the form

$$h(h-2m-4)(h-4m-6) - \left(\frac{2Z_a R}{n}\right)^2 (h-2m-2) = 0. \tag{A.2}$$

This equation has the three real and distinct roots.

The equation of the fourth degree for $h(R)$ has the form

$$\begin{aligned}(h-6m-12)\left[h(h-2m-6)(h-4m-10) - \left(\frac{Z_a R}{n}\right)^2 (7h-12m-18)\right] \\ -3\left(\frac{Z_a R}{n}\right)^2 h(h-2m-2) + 9\left(\frac{Z_a R}{n}\right)^4 = 0.\end{aligned} \tag{A.3}$$

This equation has the four real and distinct roots.

APPENDIX B

Spheroidal functions $\psi_{n_\xi n_\eta m}$ with arbitrary m and n_ξ, $n_\eta \leq 2$ in terms of spherical functions Ψ_{nlm}:

$$\psi_{00m} = \Psi_{m+1,m,m}, \tag{B.1}$$

$$\begin{aligned}\psi_{01m} &= \left[1 + \left(\frac{nh_1}{Z_a R}\right)^2\right]^{-\frac{1}{2}} \left[\frac{nh_1}{Z_a R}\Psi_{m+2,m,m} + \Psi_{m+2,m+1,m}\right], \\ \psi_{10m} &= \left[1 + \left(\frac{nh_2}{Z_a R}\right)^2\right]^{-\frac{1}{2}} \left[\frac{nh_2}{Z_a R}\Psi_{m+2,m,m} + \Psi_{m+2,m+1,m}\right],\end{aligned} \tag{B.2}$$

$$\psi_{02m} = C_{02m}\left[\sqrt{\frac{m+2}{m+1}}\frac{h_1}{h_1-4m-6}\Psi_{m+3,m,m} + \sqrt{\frac{2m+3}{m+1}}\frac{nh_1}{2Z_aR}\Psi_{m+3,m+1,m} + \Psi_{m+3,m+2,m}\right],$$

$$\psi_{11m} = C_{11m}\left[\sqrt{\frac{m+2}{m+1}}\frac{h_2}{h_2-4m-6}\Psi_{m+3,m,m} + \sqrt{\frac{2m+3}{m+1}}\frac{nh_2}{2Z_aR}\Psi_{m+3,m+1,m} + \Psi_{m+3,m+2,m}\right],$$

$$\psi_{20m} = C_{20m}\left[\sqrt{\frac{m+2}{m+1}}\frac{h_3}{h_3-4m-6}\Psi_{m+3,m,m} + \sqrt{\frac{2m+3}{m+1}}\frac{nh_3}{2Z_aR}\Psi_{m+3,m+1,m} + \Psi_{m+3,m+2,m}\right], \tag{B.3}$$

In (B.2), h_1,h_2 are the solutions of a quadratic equation and in (B.3), h_1,h_2,h_3 are the solutions of a cubic equation presented in Appendix A.

APPENDIX C

The explicit expressions of spheroidal Sturmian functions with arbitrary m and n_ξ, $n_\eta \leq 2$:

$$\psi_{00m} = e^{-\frac{\kappa R}{2}(\xi+\eta)}\left[(\xi^2-1)(1-\eta^2)\right]^{\frac{m}{2}}e^{\pm im\varphi}; \tag{C.1}$$

$$\begin{aligned}\psi_{01m} &= \psi_{00m}\left[1-\frac{\xi-1}{2}d_1^{(1)}(h_1)\right]\left[1+\frac{1+\eta}{2}d_1^{(2)}(h_1)\right],\\ \psi_{10m} &= \psi_{00m}\left[1-\frac{\xi-1}{2}d_1^{(1)}(h_2)\right]\left[1+\frac{1+\eta}{2}d_1^{(2)}(h_2)\right],\end{aligned} \tag{C.2}$$

in which $d_1^{(1,2)}(h_{1,2}) = (m+1)^{-1}[h_{1,2} - 2(m+1) \pm \kappa R]$, and h_1, h_2 are the solutions of the quadratic equation $h^2 - 2(m+1)h - (\kappa R)^2 = 0$;

$$\psi_{02m} = \psi_{00m}\left[1 - \frac{\xi-1}{2}d_1^{(1)}(h_1) + \left(\frac{\xi-1}{2}\right)^2 d_2^{(1)}(h_1)\right]$$
$$\left[1 + \frac{1+\eta}{2}d_1^{(2)}(h_1) + \left(\frac{1+\eta}{2}\right)^2 d_2^{(2)}(h_1)\right],$$
$$\psi_{11m} = \psi_{00m}\left[1 - \frac{\xi-1}{2}d_1^{(1)}(h_2) + \left(\frac{\xi-1}{2}\right)^2 d_2^{(1)}(h_2)\right]$$
$$\left[1 + \frac{1+\eta}{2}d_1^{(2)}(h_2) + \left(\frac{1+\eta}{2}\right)^2 d_2^{(2)}(h_2)\right],$$
$$\psi_{20m} = \psi_{00m}\left[1 - \frac{\xi-1}{2}d_1^{(1)}(h_3) + \left(\frac{\xi-1}{2}\right)^2 d_2^{(1)}(h_3)\right] \qquad \text{(C.3)}$$
$$\left[1 + \frac{1+\eta}{2}d_1^{(2)}(h_3) + \left(\frac{1+\eta}{2}\right)^2 d_2^{(2)}(h_3)\right],$$

in which

$$d_1^{(1,2)}(h_i) = (m+1)^{-1}[h_i - 2(2m+3) \pm 2\kappa R],$$
$$d_2^{(2,1)}(h_i) = [2(m+2)]^{-1}\left[(h_i - 2(m+2))d_1^{(2,1)}(h_i) \mp 4\kappa R\right] \qquad \text{(C.4)}$$

and h_1, h_2, h_3 are the solutions of the cubic equation $h(h-2m-4)(h-4m-6) - 4(\kappa R)^2(h-2m-2) = 0$.

REFERENCES

1. Landau, L. D.; Lifshitz, E. M. *Quantum Mechanics: Non-Relativistic Theory*, 3rd ed.; Pergamon: Oxford UK, 1977.
2. Komarov, I. V.; Ponomarev, L. I.; Slavyanov, S. Y. *Spheroidal and Coulomb Spheroidal Functions*; Moscow USSR: Nauka, 1976.
3. Coulson, C. A.; Robinson, P. D. *Proc. Phys. Soc.* **1958**, *71*, 815.
4. Robinson, P. D. *Proc. Phys. Soc.* **1958**, *71*, 828.
5. Cook, D. B.; Fowler, P. W. *Am. J. Phys.* **1981**, *49*, 857.
6. Sung, S. M.; Herschbach, D. R. *J. Chem. Phys.* **1991**, *95*, 7437.
7. Granger, B. E.; Hamilton, E. L.; Greene, C. H. *Phys. Rev. A* **2001**, *64*, 042508.
8. Kereselidze, T.; Machavariani, Z. S.; Chkadua, G. *Eur. Phys. J. D* **2011**, *63*, 81.
9. Mardoyan, L. G.; Pogosyan, G. S.; Sissakyan, A. N.; Ter-Antonyan, V. M. *J. Phys. A* **1983**, *16*, 711.
10. Kereselidze, T. M.; Noselidze, I. L.; Chibisov, M. I. *J. Phys. B: At. Mol. Opt. Phys.* **2003**, *36*, 853.
11. Shull, H.; Löwdin, P. O. *J. Chem. Phys.* **1959**, *30*, 617.
12. Avery, J.; Avery, J. *Generalized Sturmians and Atomic Spectra*; World Scientific: Singapore, 2006.

13. Shibuya, T.; Wulfman, C. *Proc. R. Soc. A* **1965**, *286*, 376.
14. Koga, T.; Matsuhashi, T. *J. Chem. Phys.* **1988**, *89*, 983.
15. Avery, J.; Avery, J. *Phys. Chem. A* **2009**, *113*, 14565.
16. Avery, J.; Avery, J. *Mol. Phys.* **2012**, *110*, 1593.
17. Avery, J. *Hyperspherical Harmonics and Generalized Sturmians*; Kluwer: Dordrecht, Netherlands, 2000.
18. Aquilanti, V.; Caligiana, A.; Cavalli, S. *Int. J. Quantum Chem.* **2003**, *92*, 99.
19. Colleti, C.; Calderini, D.; Aquilanti, V. *Adv. Quantum Chem.* **2013**, *67*, 73.
20. Kereselidze, T.; Chkadua, G.; Defrance, P. *Mol. Phys.* **2015**, *113*, 3471.
21. Kereselidze, T.; Chkadua, G.; Defrance, P.; Ogilvie, J. F. *Mol. Phys.* **2016**, *114*, 148.
22. Slavyanov, S. Y.; Lay, W. *Special Functions: A United Theory Based on Singularities*; Oxford University Press: Oxford, UK, 2000.
23. Heun, K. *Math. Ann.* **1889**, *33*, S. 161.
24. Morse, P. M.; Stueckelberg, E. C. G. *Phys. Rev.* **1929**, *33*, 932.
25. Park, D. *Z. Phys.* **1960**, *159*, 155.
26. Jaffe, G. *Z. Phys.* **1934**, *87*, 535.
27. Bates, D. R.; Reid, R. H. G. In *Advanced in Atomic and Molecular Physics*; Bates, D. R., Esterman, I., Eds.; Vol. 4, Academic: New York, USA, 1968.
28. Madsen, M. M.; Peek, J. M. *At. Data* **1971**, *2*, 171.
29. Ponomarev, L. I.; Puzinina, T. P. *Zh. Eksp. Teor. Fiz.* **1967**, *52*, 1273.
30. Aubert, M.; Bessis, N.; Bessis, G. *Phys. Rev. A* **1974**, *10*, 51.
31. Turbiner, A. V.; Olivares-Pilon, H. *J. Phys. B: At. Mol. Opt. Phys.* **2011**, *44*, 101.
32. Korobov, V. I. *Phys. Rev. A* **2000**, *61*, 064503.
33. Greene, C. H.; Dickinson, A. S.; Sadeghpour, H. R. *Phys. Rev. Lett.* **2000**, *85*, 2458.

FURTHER READING

34. Mardoyan, L. G.; Pogosyan, G. S.; Sissakyan, A. N.; Ter-Antonyan, V. M. *Teor. Mat. Fiz.* **1985**, *64*, 171.
35. Kereselidze, T. M. *Bull. Acad. Sci. Georgian SSR* **1990**, *139*, 481.
36. Kereselidze, T. M.; Machavariani, Z. S.; Noselidze, I. L. *J. Phys. B: At. Mol. Opt. Phys.* **1996**, *29*, 257.
37. Kereselidze, T. M.; Machavariani, Z. S.; Noselidze, I. L. *J. Phys. B: At. Mol. Opt. Phys.* **1998**, *31*, 15.
38. Aquilanti, V.; Cavalli, S.; Coletti, C.; Grossi, G. *Chem. Phys.* **1996**, *209*, 405.
39. Aquilanti, V.; Coletti, C. *Chem. Phys.* **1997**, *214*, 1.
40. Aquilanti, V.; Caligiana, A. *Chem. Phys. Lett.* **2002**, *366*, 157.
41. Koga, T.; Matsuhashi, T. *J. Chem. Phys.* **1987**, *87*, 4696.
42. Peek, J. M. *J. Chem. Phys.* **1965**, *43*, 3004.
43. Peek, J. M. *Phys. Rev.* **1966**, *153*, 33.
44. Power, J. D. *Phil. Trans. R. Soc. A* **1973**, *274*, 663.
45. Ishikawa, A.; Nakashima, H.; Nakatsuji, H. *J. Chem. Phys.* **2008**, *128*, 124103.